

## Exchange of Monooleoylphosphatidylcholine as Monomer and Micelle with Membranes Containing Poly(ethylene glycol)-Lipid

David Needham, Natalia Stoicheva, and Doncho V. Zhelev

Department of Mechanical Engineering and Materials Science, Duke University, Durham, North Carolina 27708-0300 USA

**ABSTRACT** Surface-grafted polymers, such as poly(ethylene glycol) (PEG), provide an effective steric barrier against surface-surface and surface-macromolecule interactions. In the present work, we have studied the exchange of monooleoylphosphatidylcholine (MOPC) with vesicle membranes containing 750 mol wt surface-grafted PEG (incorporated as PEG-lipid) from 0 to 20 mol % and have analyzed the experimental results in terms of thermodynamic and stationary equilibrium models. Micropipette manipulation was used to expose a single lipid vesicle to a flow of MOPC solution (0.025  $\mu\text{M}$  to 500  $\mu\text{M}$ ). MOPC uptake was measured by a direct measure of the vesicle area change. The presence of PEG(750) lipid in the vesicle membrane inhibited the partitioning of MOPC micelles (and to some extent microaggregates) into the membrane, while even up to 20 mol % PEG-lipid, it did not affect the exchange of MOPC monomers both into and out of the membrane. The experimental data and theoretical models show that grafted PEG acts as a very effective molecular scale “filter” and prevents micelle-membrane contact, substantially decreasing the apparent rate and amount of MOPC taken up by the membrane, thereby stabilizing the membrane in a solution of MOPC that would otherwise dissolve it.

### INTRODUCTION

When lipid bilayer vesicles are placed in surfactant solutions, both monomer and micelles can interact with the bilayer, and the mass and composition of the bilayer can be changed in seconds (Evans et al., 1994; Needham and Zhelev, 1995; Zhelev, 1996). These changes in composition have direct consequences on bilayer structure and material properties and can ultimately lead to solubilization of the lipid bilayer. Little is known at present about the physical mechanisms of bilayer disruption by solubilizing surfactants, although some new experiments have begun to measure the effects of naturally occurring detergents on membrane material properties at sub-lytic concentrations (Evans et al., 1994; Needham and Zhelev, 1995). Even less is known about how and to what extent grafted layers of polymers like poly(ethylene glycol) (PEG) at membrane surfaces can inhibit the interactions between the lipid membrane and macromolecules and association colloids like micelles. In this paper we use a micropipette technique to directly measure the exchange of lysolipids with lipid bilayer vesicles and show how the incorporation of PEG-lipids influences this exchange.

In contrast to the strong solubilizing power of the high critical micelle concentration (CMC) bile acids (Evans et al., 1994), we have found previously that the exchange of the lysolecithin monooleoylphosphatidylcholine (MOPC), did not cause lipid bilayer failure at the CMC (where the amount of MOPC in the membrane reached saturation at

approximately a few mol %) (Needham and Zhelev, 1995). At and below the CMC for this surfactant, bilayers were still cohesive structures. [Note that the CMC for this lysolipid is in the micromolar range—monomer concentrations are  $\sim 4000\times$  lower than for bile acids.] Uptake appeared to be initially limited to the outer, exposed monolayer. It was not until the bilayer was exposed to higher concentrations of MOPC, of 5  $\mu\text{M}$  to 10  $\mu\text{M}$  and above, and for longer times, did the uptake exceed monolayer capacity, lysolipid was transferred across the bilayer midplane, and the membrane eventually ruptured. Membrane concentrations of  $\sim 30$  mol % for a single vesicle were achieved before failure, which approached the solubility limit of lipid bilayers in bulk phospholipid/lysolipid mixtures (VanEchteld et al., 1981). While lysolipid monomer is not sufficient to cause bilayer failure or to solubilize the bilayer, micelles are.

In order to gain more insight into these issues of bilayer solubilization by surfactant systems, it would be useful to be able to restrict the access of micelles to the bilayer surface. We hypothesized that interactions of micelles with the bilayer could be inhibited if it were covered by a layer of grafted PEG. This hypothesis was motivated by our expanding interest in exploring the molecular scale permeability and molecular size cutoff of such polymer-grafted layers to small molecules, macromolecules, and microparticles and, in particular, by experiments that showed PEG-lipids could in fact inhibit the nonspecific binding of ovalbumin to a lipid surface (Torchilin et al., 1994) and the specific binding of avidin to a biotin “receptor” (Noppl-Simson and Needham, 1996).

An important and surprising feature that has appeared in analyzing and interpreting our results is the role that “micro aggregation” (oligomers as opposed to the usual multimeric micelles) of the surfactants in solution plays in the exchange of MOPC for concentrations that are both below and above the CMC, i.e., the colligative properties of the surfactant

Received for publication 20 May 1997 and in final form 29 July 1997.

Address reprint requests to David Needham, Department of Mechanical Engineering and Materials Science, Duke University, Durham, NC 27708-0300. Tel.: 919-660-5355; Fax: 919-660-5362; E-mail: dn@egr.duke.edu.

Dr. Stoicheva's permanent address is the Institute of Biophysics, Bulgarian Academy of Sciences, Sofia 1113, Bulgaria.

© 1997 by the Biophysical Society

0006-3495/97/11/2615/15 \$2.00

solution itself are exposed by bilayer-bulk solution exchange due to the size-dependent filtering ability of the PEG layer, even for oligomers. Although we are not aware of any previous data that show the presence of pre-CMC oligomers for MOPC per se, it is well recognized that other surfactants in bulk solution are known to form aggregates of various sizes, and the distribution of aggregate size is concentration-dependent (Evans et al., 1994; Funasaki et al., 1990; Ruckenstein and Nagarajan, 1975). As will be shown by the analysis presented in this paper, the MOPC uptake measurements provide both a measure of the CMC of the lysolipid, and allow us to detect the presence of small aggregates in the lysolipid solutions below the CMC. Interestingly then, depending on its surface density, the polymer layer can filter out not only the large "conventional" micelles but also the smaller oligomers.

With regard to the structure and steric properties of surface-grafted polymer layers, previous studies have shown that the presence of grafted polymers, such as PEG, at lipid membrane and other surfaces can provide a strong intersurface, steric repulsion (Khul et al., 1994; Klibanov et al., 1990; McIntosh et al., 1987; Tirrell et al., 1991; Yoshioka, 1991). At the molecular level, grafted PEG can also inhibit the close approach of macromolecules to a modified surface (Beddu et al., 1996; Chonn and Cullis, 1992; Jeon et al., 1991; Noppl-Simson and Needham, 1996; Torchilin et al., 1994). This inhibition of macromolecular adsorption appears to be the underlying mechanism whereby proteins (Zalipsky, 1995) and microcarrier drug delivery systems are stabilized against cellular uptake when injected into the blood stream—the so-called "stealth" effect (Allen, 1989; Allen et al., 1991; Klibanov et al., 1990; Needham et al., 1992; Papahadjopoulos et al., 1991; Torchilin et al., 1994; Torchilin and Papisov, 1994; Wu et al., 1993) (for reviews see Huang, 1992; Lasic and Martin, 1995; and references therein). Modeling of this grafted polymer has shown that, depending on the molecular weight of the polymer and its surface density, at least two distinguishable regimes can be identified, namely, "mushrooms" (isolated grafts) and "brushes" (extended chain conformation determined by the interactions between neighboring chains) (Carignano and Szeleifer, 1994; Chakrabarti and Toral, 1990; deGennes, 1980; Wijmans et al., 1992). Thus, depending on the concentration regime (mushroom or brush), a surface will be expected to have a greater or lesser "permeability" to the adsorption of molecular and macromolecular species of a given size and surface interaction. For example, it has been found that the nonspecific binding of ovalbumin to liposomes was inhibited by  $\sim 1$  mol % of a PEG-lipid with a molecular weight of 5,000 (Torchilin et al., 1994). Similarly, in the avidin-biotin binding experiments of Noppl and Needham (Noppl-Simson and Needham, 1996), it was demonstrated that even a relatively small 750-mol wt polymer, at relatively low surface density ( $\sim 10$  mol %), extending only 2.5 nm from the lipid bilayer surface (Kenworthy et al., 1995), could inhibit the access of a macromolecule of only a few nanometers in dimension.

The goal of the present experiments was to determine to what extent grafted water-soluble polymer might selectively inhibit the interaction of lysolipid monomer and micelles with lipid bilayer surfaces. We have studied the exchange of the lysolipid, MOPC, with vesicle membranes containing the same 750-mol wt PEG-lipid. Because lysolipid micelles are of a similar size to avidin, it might be expected that the access of micelles, and to a lesser extent monomers, to the surface of the lipid bilayer will similarly depend strongly on the surface density of the polymeric barrier at the bilayer interface, and may even be inhibited. Given this general feature, there are likely to be differences between the exchange of an avidin macromolecule and the micellar association colloid. Unlike the adsorption of avidin, where the macromolecule binds to its biotin "receptor" and does not desorb during the course of an experiment (its off rate is  $\sim 3$  months $^{-1}$ !), MOPC monomer uptake and micelle-membrane "fusion" are coupled with the rapid desorption of MOPC monomers from the bilayer back to the bulk solution (Needham and Zhelev, 1995). This coupling between uptake and desorption establishes a stationary equilibrium concentration of MOPC in the membrane. This stationary MOPC concentration is uniquely measured in the micropipette experiment by a corresponding vesicle area change, and so provides a direct assay for the dependence of MOPC exchange with the bilayer on the presence of grafted polymer and MOPC bulk solution concentration. The experimental results are discussed in terms of a model, where monomer uptake and micelle-membrane fusion are considered an apparent first-order rate reaction, and the activation energy for species access and uptake by the lipid bilayer is increased due to the work to create free area (polymer-denuded) at the membrane surface. A thermodynamic analysis, following the work of Evans (Evans et al., 1994), is also used to test for ideality of mixing in both aqueous and bilayer phases.

## MATERIALS AND METHODS

### Vesicle preparation

Lipid vesicles were made from 1-stearoyl-2-oleoyl-*sn*-glycero-3-phosphocholine (SOPC) and 1,2-dimyristoyl-*sn*-glycero-3-phosphoethanolamine-*N*-PEG-750 [PEG(750)-lipid] (Avanti Polar Lipids Inc., Alabaster, AL) by using the procedure described elsewhere (Needham and Zhelev, 1996). Briefly, chloroform solutions of the particular lipids were mixed to obtain the desired molar ratios. Thirty microliters of a lipid solution were spread onto a roughened Teflon disk and the chloroform evaporated under nitrogen. Last traces of solvent were removed by placing the disk in an evacuated desiccator for 2 h (Needham and Nunn, 1990). The so-formed dried lipid layers were prehydrated with water vapor in a nitrogen carrier gas and then fully hydrated overnight with a sucrose solution at 40°C. The osmolarity of the solution was 200 mOsm. Both the pure SOPC and SOPC/PEG(750)-lipid vesicles were resuspended in a glucose solution of 205 mOsm and then used in the micromanipulation experiments.

The exchanged molecule was the lysolipid MOPC (Avanti Polar Lipids, AL). In order to prepare the lysolipid solution, a chloroform solution of the lysolipid (0.05 mg/ml) was dried under nitrogen in a vial. Then, the dried lysolipid was hydrated overnight in a glucose solution to give the final desired concentration of MOPC. The osmolarity of the hydrating solution

was 205 mOsm, the same as the glucose solution that was used for resuspending the vesicles in the microscope chamber.

## Micromanipulation

The experimental chamber was 3 mm thick and open at both sides for micromanipulation. Experiments were performed at room temperature (23°C) using an inverted Nikon microscope with a 60× oil immersion objective. The microscope images were recorded using a COHU CCD camera. The micropipettes were made of 0.75 capillary glass tubing pulled to a fine point with a vertical pipette puller and cut to the desired diameter with a microforge. The pipettes were connected to a manometer system that allowed the applied pressures to be changed and measured to an accuracy of 2  $\mu$ atm. The micropipette suction pressures were measured by differential transducer (Validyne DP15–24). The measured pressures together with real time were multiplexed on the recorded images with a multiplexer (Model 401, Vista Electronics, La Mesa, CA). The recorded images were used to measure the change of the vesicle projection length inside the holding pipette during uptake and desorption of lysolecithin, and to calculate the membrane tension. This was done by using calibrated video calipers (Model 305, Vista Electronics).

## Experimental

The micropipette assay used here for studying the exchange of MOPC with SOPC vesicles with and without grafted PEG(750) was similar to the one used by Needham and Zhelev (1995), and is illustrated in Fig. 1. The

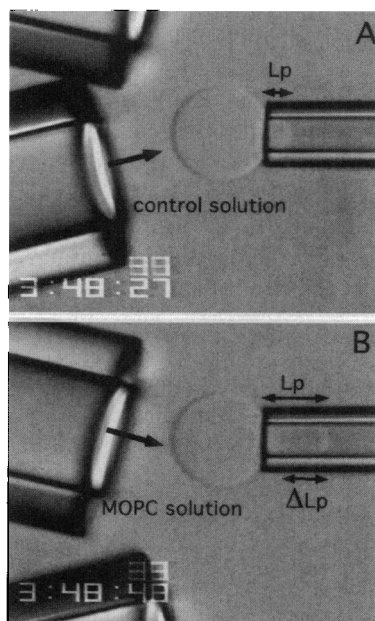


FIGURE 1 Videomicrograph showing arrangement of the holding pipette and the two flow pipettes that deliver MOPC and MOPC-free solution at a controlled flow rate to the test vesicle. (A) Initial vesicle projection length ( $L_p$ ) inside the pipette is established when the lower pipette is used to flow MOPC-free bathing solution over the vesicle; (B) the lower pipette is replaced by the upper pipette and MOPC solution is made to flow over the vesicle, causing an increase of the vesicle projection length. Exchanging the pipettes once more, and flowing the bathing solution over the vesicle, returns the projection length back to its original position as in (A). The whole experiment is recorded on videotape and analyzed later to produce plots of  $L_p$  versus time.  $\Delta L_p$  is converted to fractional area change of the vesicle which in turn is converted to mol % MOPC taken up into the vesicle membrane (see text for details).

holding pipette was preincubated in a solution of 1 wt % bovine serum albumin (Sigma Chemical Co., MO) before any experiment. This treatment minimized vesicle adhesion to the pipette wall. Three micropipettes were mounted on the microscope stage. A single vesicle was held by the holding pipette with a suction pressure of 200 N/m<sup>2</sup> (2000 dyn/cm<sup>2</sup>) in a bathing, MOPC-free solution (Fig. 1 A). This suction pressure was sufficient to keep the vesicle in the pipette, and induced only low levels of tension ( $\sim$ 0.2 mN/m) in the vesicle membrane compared to the tensile strength of the membrane ( $\sim$ 6 mN/m for pure SOPC, and less than this for MOPC-rich bilayers) (Needham and Nunn, 1990). [In these exchange experiments where the molecular composition of the membrane was changed by the incorporation of lytic surfactants, the tensile strength of the membrane is dramatically reduced by MOPC (McIntosh et al., 1995) and, for high CMC surfactants, can eventually go to zero at the CMC of the surfactant (Evans et al., 1994). It was therefore important to keep as low a tension on the vesicle as possible to achieve equilibrium uptake without premature failure of the vesicle.] The same solution as in the bathing solution was blown over the vesicle, from the lower blowing pipette, to establish initial starting conditions (Fig. 1 A). MOPC was delivered to the test vesicle by exchanging the lower pipette for the upper pipette and blowing an osmotically matched test solution of desired concentration of MOPC (Fig. 1 B). After exposure to MOPC-containing solution, any uptake of MOPC by the lipid vesicle was detected by an increase in the projection length ( $L_p$ ) of the vesicle in the micropipette, as shown in Fig. 1 B. For a vesicle of constant volume, this increase in projection length represented an increase in vesicle membrane area. As discussed below (Eq. 1), this area change was then converted to a mol % of MOPC in the membrane (Needham and Zhelev, 1995; Zhelev, 1996). With time, the vesicle area either reached a maximum or the vesicle broke down. Then, to desorb the MOPC from an intact vesicle, the upper blowing pipette was moved away and was replaced by the lower pipette, which exposed the vesicle once more to the bathing solution (i.e., back to the arrangement in Fig. 1 A). This exposure of the MOPC-containing vesicle to lysolipid-free solution resulted in a rapid decrease of the membrane projection length and a minimum final area. This minimum final area was similar to, if not the same as, the vesicle area before MOPC uptake, indicating essentially complete desorption of lysolipid, and demonstrating reversible exchange. The measured projection lengths, together with the measured pipette radius and the outside vesicle radius, were used to calculate the original vesicle area,  $A_o$ , and the area change due to MOPC uptake,  $\Delta A$  (Kwok et al., 1980). Assuming that, at least initially, MOPC only entered the outer monolayer, the relative fractional area change  $\Delta A/A_o$  was converted to a mol % for exchanged MOPC molecules relative to the total number of lipids in the bilayer by using the approximation,

$$\text{mol\%MOPC}_{\text{bilayer}} = \frac{\Delta A}{A_o} \frac{A_{\text{SOPC}}}{A_{\text{MOPC}}} \times 100 \quad (1)$$

where  $\Delta A$  is the change in vesicle area due to MOPC uptake relative to the starting area  $A_o$ ;  $A_{\text{SOPC}}$  is the area per lipid molecule of 67  $\text{\AA}^2$ ; and  $A_{\text{MOPC}}$  is the area per MOPC molecule (projected area of the acyl chain) of 35  $\text{\AA}^2$  (Zhelev, 1996).

Since the CMC of MOPC is expected to represent an important discontinuity in the behavior of surfactant solutions, an independent measurement of the CMC for MOPC was made by a fluorescence technique (Chattopadhyay and London, 1984). Briefly, a series of solutions were made up that contained increasing concentrations of MOPC in the range  $10^{-7}$  to  $10^{-4}$  M. Diphenyl hexatriene (DPH), a lipid-soluble fluorescent dye, was added to these samples and the intensity of fluorescence was measured by spectrofluorimeter at absorption and emission wavelengths of 358 nm and 430 nm, respectively (Aminco Bowman, Series 2, Luminescence Spectrometer). The CMC was determined by plotting the fluorescence intensity (in arbitrary units) versus concentration of MOPC solutions, made up by diluting a 100 mM stock solution of MOPC (solubilized initially by tetrahydrofuran) in water (Chattopadhyay and London, 1984). The CMC was estimated from the point at which the slope of a plot of intensity versus concentration showed a sharp increase corresponding to a fluorescence

increase due to micelle formation and the solubilization of increasing amounts of DPH dye.

Three distinct experimental measurements were performed using the micropipette manipulation technique:

1. *MOPC uptake as a function of PEG-lipid concentration.* Bilayer uptake and desorption of MOPC were measured as a function of PEG(750)-lipid membrane concentration from 0 to 20 mol % PEG(750)-lipid upon exposure to 3  $\mu\text{M}$  or 100  $\mu\text{M}$  MOPC solutions.
2. *MOPC uptake as a function of MOPC bulk solution concentration.* MOPC uptake was measured as a function of MOPC concentration in the bathing solution from 0.025  $\mu\text{M}$  to 500  $\mu\text{M}$  MOPC for 4 mol % PEG(750)-lipid bilayers; measurements were also made for 20 mol % PEG(750)-lipid bilayers at 0.025  $\mu\text{M}$  to 100  $\mu\text{M}$  MOPC. MOPC uptake by unmodified bilayers was also made at the CMC of 3  $\mu\text{M}$ .
3. *Membrane mechanical strength as a function of membrane MOPC content.* Mechanical tests of bilayer tensile strength were carried out on vesicles that contained various amounts of PEG(750)-lipid as a function of the amount of MOPC in the membrane.

## RESULTS

The Results section is divided into two parts: the first part (A) presents the experimental results, and the second part (B) presents the thermodynamic and stationary equilibrium models that were used to analyze the data.

### A. Experimental data

#### A1. Critical micelle concentration

The cross-over in fluorescence intensity between two distinct regions of the DPH fluorescence intensity versus MOPC concentration gave an estimate of the CMC for MOPC of  $2.8 \mu\text{M} \pm 0.8 \mu\text{M}$ , which for all intents and purposes is rounded up to 3  $\mu\text{M}$ .

#### A2. MOPC uptake: demonstration of the basic effect

The basic effect of how high bathing concentrations of MOPC can result in uptake of MOPC into the bilayer and ultimately vesicle rupture is shown in Fig. 2. Also shown in Fig. 2 is the inhibition of the MOPC-induced bilayer rupture when PEG-lipid is included in the bilayer.

When an unmodified vesicle was exposed to a 100  $\mu\text{M}$  MOPC solution, the vesicle area rapidly increased, signifying rapid partitioning of MOPC into the lipid bilayer. This resulted in bilayer rupture at  $\sim 16$  mol %, consistent with previous studies in which MOPC was exchanged with egg PC vesicles (Needham and Zhelev, 1995; Zhelev, 1996). In contrast to the unmodified SOPC vesicles, the presence of 20 mol % PEG(750)-lipid completely prevented rupture when the vesicle was exposed to 100  $\mu\text{M}$  MOPC. The amount of MOPC taken up by the membrane increased rapidly, but then eventually reached a plateau at 5–6 mol % MOPC, representing equilibrium uptake of MOPC into the outer monolayer of the bilayer (Needham and Zhelev, 1995; Zhelev, 1996). This level of uptake was found to be essentially identical to that for the same 20 mol % PEG-lipid vesicle exposed to the CMC of MOPC, 3  $\mu\text{M}$ .

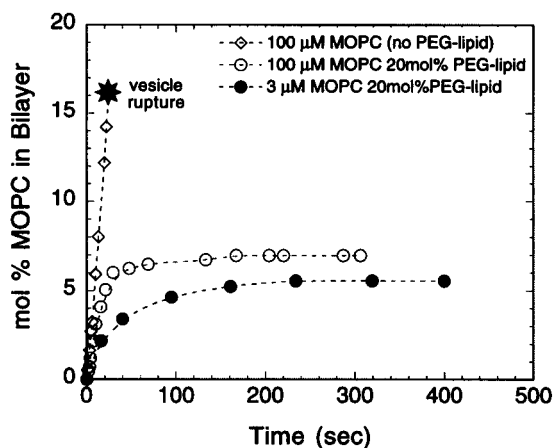


FIGURE 2 Exposure of single SOPC vesicles to a flow of MOPC solution. Open diamonds, SOPC (no PEG-lipid) and 100  $\mu\text{M}$  MOPC; open circles, 20 mol % PEG-lipid and 100  $\mu\text{M}$  MOPC; filled circles, 20 mol % PEG-lipid and 3  $\mu\text{M}$  MOPC. Without PEG-lipid in the bilayer, exposure to 100  $\mu\text{M}$  MOPC causes rapid expansion and rupture of the membrane. With 20 mol % PEG-lipid in the bilayer, uptake in 100  $\mu\text{M}$  MOPC is essentially the same as that observed at the CMC (3  $\mu\text{M}$ ) and bilayers are stable. Dotted lines are simply curve fits through the data.

This result implied that the presence of a saturating amount (20 mol %) of PEG(750)-lipid in the lipid vesicle bilayer decreased the transport of micelles to the vesicle surface and therefore apparently eliminated the partitioning of MOPC micelles into the bilayer at elevated bulk solution concentrations that would otherwise dissolve the vesicle. The initial inference is that only monomeric species of MOPC can pass through the thin (25 Å) (Kenworthy et al., 1995) polymer layer, even when there is a large excess concentration of micelles in the bathing medium.

#### A3. MOPC uptake as a function of PEG(750)-lipid

Experiments were then carried out to determine the rate and magnitude of uptake of MOPC from 100  $\mu\text{M}$  solutions as the concentration of PEG(750)-lipid in the membrane was increased from 0.5 mol % to 20 mol % PEG-lipid. Plotted in Fig. 3, A and B are typical uptake time courses obtained for single vesicles at each PEG-lipid concentration for 100  $\mu\text{M}$  and 3  $\mu\text{M}$  MOPC, respectively. The uptake experiments were performed several times at each concentration and the standard deviation for these runs is shown on the last time point. The data are fitted with exponential curves that represent uptake of MOPC into the outer monolayer of the bilayer as described earlier by Zhelev (1996). Exposure of vesicles containing zero (Fig. 2) and 0.5 mol % (Fig. 3 A) PEG-lipid to 100  $\mu\text{M}$  MOPC resulted in breakage of the membranes before they could approach any stationary equilibrium. For these absent and low surface densities of PEG-lipid, the presence of micelles in the bathing solution produced rapid uptake of MOPC, causing vesicle breakage. However, for PEG(750)-lipid concentrations between 1 mol % and 20 mol %, the amount of lysolipid partitioning into

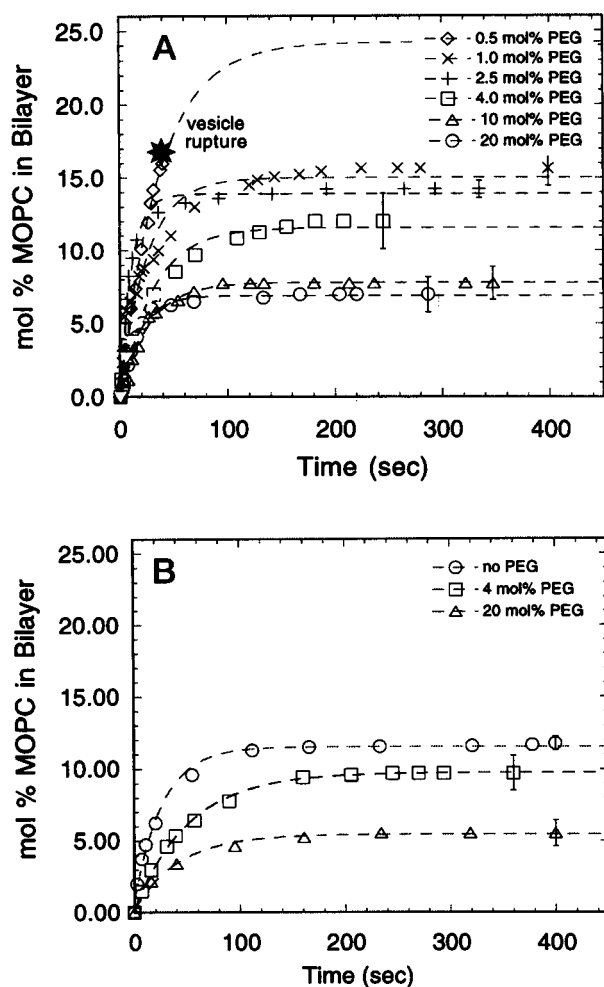


FIGURE 3 Exposure of single SOPS vesicles containing different concentrations of PEG(750)-lipid. (A) 0.5, 1, 2.5, 4, 10, and 20 mol % PEG(750)-lipid to a flow of 100  $\mu\text{M}$  MOPC solution, and (B) 0, 4, and 20 mol % PEG(750)-lipid to a flow of 3  $\mu\text{M}$  MOPC solution. The data are fitted with an exponential that represents uptake into the outer monolayer of the bilayer (Zhelev, 1996). SD shown on the last data point for each concentration are averages of 10 test vesicles.

the membrane reached a stationary equilibrium. The value of this equilibrium partitioning decreased monotonically with increasing PEG(750)-lipid concentration and bilayers remained stable. The apparent rate of lysolipid uptake ranged from  $0.125\text{ s}^{-1}$  to  $0.025\text{ s}^{-1}$  without any direct correlation with PEG concentration. In fact, the apparent rate of MOPC uptake was more sensitive to the rate of flow of the bathing solution than to the PEG-lipid concentration in the vesicle membrane (data not shown). [This dependence of the apparent rate of uptake on the hydrodynamic conditions is a result of the significant contribution of the rate of molecular transport across the stagnant layer to the measured rate of uptake. For the flow rates used in these experiments this contribution can be 20% or more (Zhelev, 1996).]

Uptake experiments were also carried out for MOPC solution concentrations of 3  $\mu\text{M}$ , i.e., at the CMC, for

PEG-lipid concentrations of 0, 4, and 20 mol %. These data are shown in Fig. 3 B. For this MOPC concentration, micelles were essentially absent and uptake values were consistently lower at each PEG-lipid concentration than for exposure to 100  $\mu\text{M}$  MOPC. For the 0 mol % PEG-lipid membrane, uptake at the CMC did not destroy the membrane but produced a stationary concentration of  $\sim 11$  mol % MOPC in the bilayer. With increasing PEG-lipid, the amount of MOPC uptake in the bilayer again decreased to  $\sim 5$ –6 mol %. At 20 mol % PEG-lipid, the stationary equilibrium was the same as for 100  $\mu\text{M}$  MOPC, indicating that, at 20 mol % PEG(750)-lipid, uptake for the 100  $\mu\text{M}$  case was presumably reduced to just monomer exchange.

These results for exposure of single lipid vesicles to 100  $\mu\text{M}$  and 3  $\mu\text{M}$  MOPC solutions are summarized in Fig. 4, where the average stationary equilibrium uptake values are presented over the whole range of PEG-lipid membrane concentrations studied (0–20 mol % PEG-lipid). From these data it is clear that the amount of MOPC partitioning into the vesicle membrane at stationary equilibrium is strongly reduced by increasing the amount of PEG(750)-lipid in the bilayer, and at 20 mol % PEG(750)-lipid, only monomer appears to be able to gain access to the bilayer.

#### A4. MOPC desorption from loaded bilayers

As Needham and Zhelev (1995) and Zhelev (1996) have shown previously, the desorption, or wash-out, of the lysolipid from MOPC-rich membranes involves only monomers and occurs very rapidly upon exposure of the MOPC-loaded bilayers to MOPC-free solution. Fig. 5 shows again the time-dependence for MOPC uptake followed by its desorp-

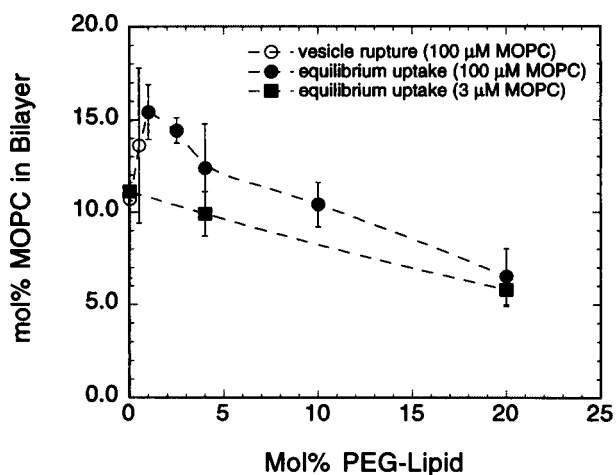


FIGURE 4 Stationary equilibrium uptake of MOPC into SOPS vesicles versus mol % PEG-lipid in the vesicle membrane for bulk solution concentrations of MOPC of 3  $\mu\text{M}$  (i.e., at the CMC) and 100  $\mu\text{M}$ . Standard deviations are averages of 10 vesicles at each concentration. Open circles, 100  $\mu\text{M}$ , vesicles broke before reaching equilibrium. Filled symbols, vesicles were stable in MOPC solutions of MOPC and reached equilibrium uptake. Closed circles, 100  $\mu\text{M}$ ; closed squares, 3  $\mu\text{M}$ . Dotted lines are simply curve fits through the data.

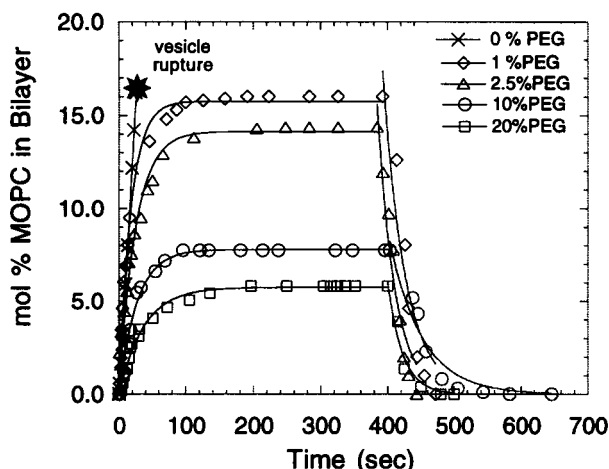


FIGURE 5 Uptake and desorption of MOPC by single SOPC vesicles after exposure to ( $100 \mu\text{M}$ ) MOPC solutions ( $>5 \text{ min}$ ) for different mol % of PEG(750)-lipid, 0, 1, 2.5, 10, and 20 mol %. Solid lines are theoretical fits to the data (Zhelev, 1996).

tion for individual vesicle experiments with different concentrations of PEG(750)-lipid. As shown earlier (Fig. 2) at 0 mol % PEG(750)-lipid, vesicles exposed to  $100 \mu\text{M}$  MOPC broke after only 50 s, stationary equilibrium was not reached, and so desorption experiments could not be carried out. At 1, 2.5, 10, and 20 mol % PEG(750)-lipid, test vesicles remained intact, the uptake with time reached a constant value, and desorption of the MOPC was then measured by the reduction in the projection length ( $L_p$ ) of the vesicle membrane inside the pipette. For a flow rate of bathing solution of  $400 \mu\text{m/s}$ , the measured overall rates of desorption from these data are in fact similar for all PEG(750)-lipid concentrations and have an average value of  $0.4 \pm 0.2 \text{ s}^{-1}$  (measured from five vesicles at each PEG-lipid concentration). This value is similar to the one measured in the experiment of Needham and Zhelev (1995) of  $0.2 \text{ s}^{-1}$  (at the slightly slower flow rate of  $300 \mu\text{m/s}$ ) for desorption of MOPC from unmodified egg PC membranes. Again, desorption rates are very sensitive to flow rates of solutions over the vesicle surface. Solid lines are theoretical fits according to the analysis of Zhelev (1996). Because of the small size of the MOPC monomer, it might be expected that the kinetics of exchange will not be affected by the presence of PEG(750)-lipid. It is in fact seen from the data that the kinetics of MOPC desorption as monomer was not significantly affected by the presence of PEG-lipid over the whole range of PEG surface densities, i.e., high densities of PEG(750)-lipid did not decrease the *off* rate of the monomer from the bilayer.

Taken together, these uptake and desorption results demonstrate that at membrane concentrations of PEG(750)-lipid above 1 mol %, micelle-membrane fusion begins to be reduced and at 20 mol % PEG(750)-lipid this process is almost completely inhibited. However, the dense, 20 mol % PEG layer does not retard the desorption of monomer from the membrane into solution, (as shown in Fig. 5) and, by

implication, the *on* rate of monomer from solution to the membrane. There is, therefore a molecular size cutoff for MOPC transport through the 25-Å-thick PEG-lipid layer somewhere between the dimensions of the monomer and the micelle that can, in principle, be controlled by the surface density of PEG.

#### A5. MOPC bulk solution concentration

The observations that micelles can be excluded to a greater or lesser extent dependent on PEG-lipid concentration suggests that, for a given PEG-lipid mol %, there should be a sharp discontinuity in uptake as a function of bulk MOPC solution concentration around the CMC. This prompted us to measure MOPC uptake by the bilayer (strictly, into the outer monolayer of the bilayer) as a function of bathing MOPC concentration for fixed PEG-lipid concentrations of 0 mol %, 4 mol %, and 20 mol % PEG-lipid. The results are presented in Fig. 6, A and B. Measuring the concentration dependence in this way provides an opportunity to study the thermodynamic equilibrium of monomer exchange below the CMC (in the absence of micelles) and to examine the ideality of mixing of MOPC in the membrane and bulk solution following the approach by Evans (Evans et al., 1994).

The unmodified bilayer showed an uptake of MOPC into the outer monolayer of  $\sim 11 \text{ mol } \%$  when exposed to a bulk MOPC solution concentration of  $3 \mu\text{M}$  (Fig. 6 A). At bathing solution concentrations that were significantly above the CMC the bilayers rapidly broke, and so for the bare membrane no equilibrium uptake values could be obtained much beyond the CMC.

For the 4 mol % PEG-lipid composition, the amount of MOPC uptake was measured for concentrations below the CMC (0.025, 0.05, 0.1, 0.5,  $1 \mu\text{M}$ ), at the CMC ( $3 \mu\text{M}$ ), and above the CMC (10, 50, 100, 200, and  $500 \mu\text{M}$ ). Fig. 6 A shows how the amount of MOPC taken up by the 4 mol % PEG-lipid bilayer increased rapidly for MOPC concentrations from  $0.025 \mu\text{M}$  to  $3 \mu\text{M}$ , but then showed a weaker dependence on bathing concentration, above the CMC, even up to  $500 \mu\text{M}$ , where bilayers were stable for several minutes but then spontaneously broke under low pipette suction pressure.

For the 20 mol % PEG-lipid at MOPC solution concentrations of 0.025, 1, 3, 10, and  $100 \mu\text{M}$ , the initial steep rise in membrane MOPC was again seen below the CMC, but the stationary equilibrium uptake of MOPC by the membrane was significantly smaller than that for the lower PEG density of 4 mol %, indicating that the higher surface density of PEG excluded more of the micellized MOPC.

Fig. 6 B shows an expanded view of the lower concentration region of 6 A. The cross-over in slope is seen to occur at approximately the CMC of  $\sim 3 \mu\text{M}$  for both the 4 mol % PEG-lipid and 20 mol % PEG-lipid membranes, and so coincides with the micellization of the lysolipid. It is important to note that below the CMC the amount of MOPC taken up by the membrane does not increase linearly with

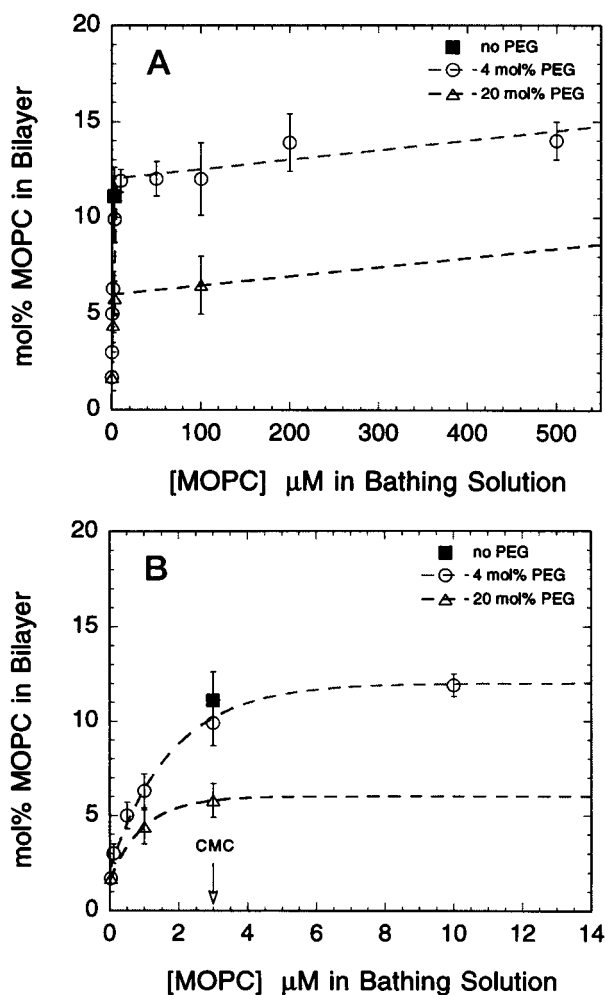


FIGURE 6 (A) Dependence of MOPC uptake into vesicles containing 0 mol % (filled square), 4 mol % (open circle), and 20 mol % (open triangle) PEG-lipid as a function of the bathing MOPC solution concentration for the whole concentration range of 0.025  $\mu$ M to 500  $\mu$ M MOPC. (B) Same data as in A, but for the low MOPC concentration range of 0.025  $\mu$ M to 20  $\mu$ M. The cross-over of the two concentration regimes occurs close to 3  $\mu$ M, the CMC of MOPC measured by DPH fluorescence. Dotted lines are simply curve fits through the data.

increasing MOPC aqueous solution concentration, but is somewhat curved. Also, there is a clear disparity between uptake for no PEG, 4 mol % PEG, and 20 mol % PEG membranes not just above the CMC but also below it.

#### A6. Mechanical tests of bilayer tensile strength

Finally in this experimental section, it is expected that as a lipid bilayer takes up more and more of a water-soluble second component (e.g., bile acid or MOPC), it will become weaker and softer (Evans et al., 1994; Needham and Zhelev, 1995; Zhelev, 1996). To test this we measured the tensile rupture strength of vesicles containing various amounts of MOPC at stationary equilibrium. Fig. 7 shows how the rupture strength of the vesicle membrane does in fact decrease with increasing amount of MOPC in the bilayer. In

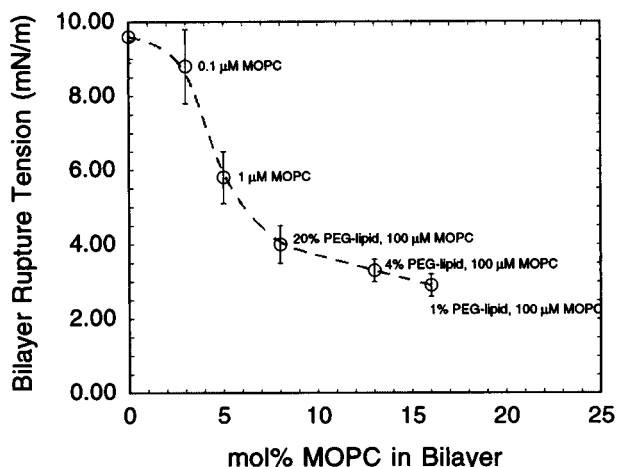


FIGURE 7 Rupture tension of vesicle membranes as a function of the mol % MOPC in the bilayer. The different amounts of MOPC in the bilayers were achieved by various combinations of bathing solution concentration and PEG-lipid in the membranes as indicated next to each data point on the plot.

order to obtain a wide range of concentrations of MOPC in the bilayer, several different combinations of lipid, PEG-lipid, and MOPC solution concentrations were used, as indicated next to each data point. Interestingly, bilayers with 1 mol % PEG-lipid exposed to 100  $\mu$ M MOPC containing 15 mol % MOPC were still relatively stable, with rupture tensions of  $\sim$ 3 mN/m. This contrasts with the uptake of the higher CMC bile acid (Evans et al., 1994), where the elastic expansion modulus and the tensile strength both went to zero at the CMC.

Since PEG-lipids were used in some but not all of these vesicle tests, we also checked to see whether the incorporation of the PEG-lipids (DMPE-PEG750) themselves had any effect on the tensile strength of the lipid vesicles. A priori it might be expected that either 1) the slightly shorter acyl chain of the DMPE-PEG lipid would reduce the tensile strength of the bilayer, since DMPC lipid vesicles have a lower tensile strength than SOPC (Needham and Evans, 1988); and/or 2) that the PEG-lipid chain may exert a lateral expanding pressure that pre-stresses the bilayer, so reducing the amount of applied stress needed to cause failure in tension (Hristova and Needham, 1994). Fig. 8 shows that this particular PEG(750)-lipid did not reduce the tensile strength significantly, up to 20 mol % PEG-lipid.

## B. Thermodynamic analysis and stationary equilibrium model

### B1. Thermodynamic analysis: dependence of MOPC uptake on MOPC solution concentration below the CMC

Before presenting the stationary equilibrium model, we consider first a thermodynamic approach to describe how the amount of MOPC taken up by the membrane depends on the aqueous solution concentration of MOPC, for conditions under which the bilayer-solution system can come to true

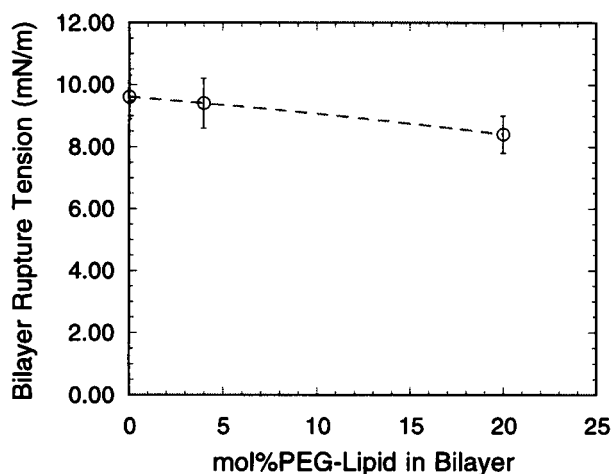


FIGURE 8 Rupture tension of vesicle membranes as a function of the mol % PEG-lipid (DMPC-PEG750) in the bilayer.

thermodynamic equilibrium. This only occurs for low PEG-lipid concentrations and MOPC solution concentrations below the CMC. Above the CMC, and for high surface densities of PEG-lipid (>10 mol %) a true thermodynamic analysis is not appropriate because micelles are kinetically trapped. Analysis of our experimental results for uptake below the CMC for 4 mol % PEG-lipid provides an indication of the ideality of mixing of MOPC in the bulk solution and in the membrane (Evans et al., 1994). A first approximation would treat the MOPC solution as monomer. Any self-association or microaggregation of MOPC in either the bulk solution and/or bilayer phases would produce deviations from this ideal approximation.

The simplest thermodynamic approach is to assume that there is only one chemical potential in the system, that of the MOPC monomer, i.e., the phospholipid is virtually insoluble and so is not exchanged, at least not initially [although phospholipid exchange with micelles would appear to be involved in the ultimate dissolution of the membrane (Evans et al., 1994)]. The balance of chemical potentials for the monomer in the bulk solution and the membrane (Evans et al., 1994) can be written in a simplified form,

$$\ln(x_m) = \frac{n_m}{n_s} \cdot \ln[x_s] + \text{constants} \quad (2)$$

where,  $x_m$  is the mol fraction of MOPC in the membrane,  $x_s$  is the mol fraction of MOPC in the bulk solution, and the *constants* term contains the reference chemical potentials and excess energy due to applied membrane tension. The prefactor in this relationship,  $n_m/n_s$ , is the ratio of monomer aggregate number in the bilayer to the number in aqueous solution, and so any value different from 1:1 indicates non-ideality of mixing and microaggregate formation.

As discussed earlier, the mol fraction of MOPC in the membrane is measured directly from the relative vesicle area change produced by exposure to MOPC. Since the mol fraction of MOPC in solution is proportional to the solution

concentration, the slope of a plot of the data from Fig. 6 as  $\ln(\text{mol fraction in the membrane})$  versus  $\ln(\text{MOPC solution concentration})$  gives  $n_m/n_s$ , the ratio of aggregation states of monomer in the bilayer to that in the solution, Fig. 9. Including 4 mol % PEG-lipid in the bilayer allowed us to carry out a full concentration dependence for uptake over a wide range of MOPC solution concentrations, up to 500  $\mu\text{M}$ . However, as discussed above, thermodynamic analysis was limited to MOPC concentrations below the CMC. As also shown in Fig. 6 B, MOPC uptake at the CMC was virtually the same for bare membranes as it was for membranes containing 4 mol % PEG-lipid, and so a coverage of 4 mol % PEG-lipid did not impede the attainment of equilibrium for the monomer species and we can apply the thermodynamic model to uptake by this membrane. The  $n_m/n_s$  ratio is 1:3 (from a least-squares best fit), indicating that there is indeed some association of monomers in the aqueous solution. If MOPC in the membrane is assumed to be monomeric and ideally dissolved in the "lipid solution" of the membrane, then, in aqueous solution, the MOPC monomers are aggregated, on average, as trimers.

This analysis then confirms the expectation that the bulk MOPC solution contains oligomers below the CMC. In corroboration of this result, Evans et al. have found previously that bile acids were also aggregated below the CMC as dimers or tetramers (Evans et al., 1994). These oligomers may also be expected to persist above the CMC. Returning to Fig. 6 B, we now have an explanation for the reduced uptake by the 20 mol % PEG-lipid membrane compared to the 4 mol % PEG-lipid membrane, despite the fact that there are no micelles in the solution. The discrepancy is due to the exclusion of oligomers by the high PEG-lipid concentration. This observation of oligomer formation will be important

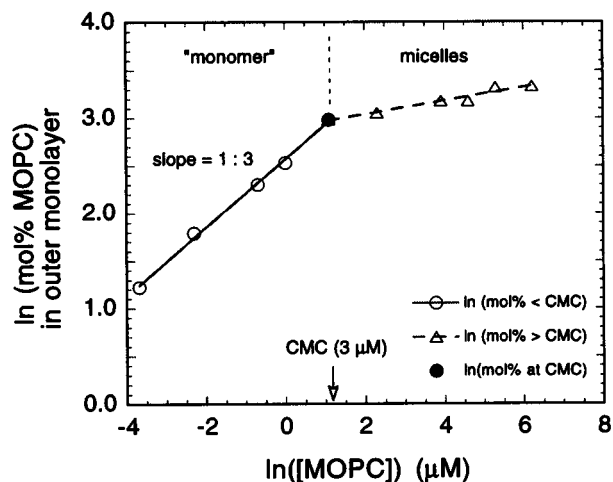


FIGURE 9 Logarithm of the mol % MOPC in the outer monolayer of the bilayer at stationary equilibrium uptake as a function of the logarithm of the concentration of MOPC in the bathing medium ( $\mu\text{M}$ ). Data are shown for 4 mol % PEG-lipid below the CMC (*open circles*), at the CMC (*filled circle*), and above the CMC (*open diamonds*). Below the CMC, the slope is 1:3, indicating deviation from 1:1 ideality, and demonstrating that MOPC forms oligomers below the CMC.



for analysis of the stationary equilibrium model in the next section, and the interpretation of the role of PEG in inhibiting the uptake of MOPC as monomers, oligomers, and micelles.

### B2. Stationary equilibrium model: effect of PEG-lipid concentration

The key finding from the data presented so far is that the presence of only a few mol % of PEG(750)-lipid in the vesicle membrane substantially inhibits the partitioning of MOPC micelles into the membrane, (up to 500  $\mu\text{M}$  solution concentration, see Fig. 6 A) and thereby prevents lysis of the membrane. However, even up to 20 mol % PEG-lipid, it does not affect significantly the exchange of MOPC true monomers out of the membrane (Fig. 5) and, by implication, into the membrane. Moreover, as has been suggested by the MOPC solution concentration dependence for 0, 4, and 20 mol % PEG-lipid (Fig. 6), and the thermodynamic analysis (Fig. 9), the PEG-graft acts to selectively sample the aggregate distribution of the surfactant solution itself, and MOPC exchange appears to involve not only monomers and micelles, but also, oligomers.

In developing the stationary equilibrium model, then, three species needed to be considered—true monomers, oligomers, and micelles. The amount of MOPC partitioning into a lipid membrane is therefore determined by a balance between MOPC taken up as both monomer, oligomer and micelle, and the desorption of true monomers (Needham and Zhelev, 1995; Zhelev, 1996). As we will discuss later, there is only one point at which, irrespective of MOPC solution concentration, true monomer is the only adsorbing species, and that is at the high, 20 mol % PEG-lipid concentrations. At all other PEG-lipid concentrations, oligomers and micelles appear to gain access to the membrane to a greater extent the lower the PEG surface density. Because it is not possible to distinguish between true monomer and oligomer (except in the high PEG-lipid case), in much of the discussion to follow, true monomers and oligomers are grouped under the italicized title of *monomer*. The task now is to evaluate how two independent parameters, namely, the concentration of PEG-lipid in the bilayer and the concentration of MOPC in the bathing aqueous solution, determine the stationary equilibrium concentration of MOPC in the bilayer through the action of these three species and the retarding influence of PEG on their exchange with the bilayer membrane.

The coupling of *monomer* uptake and micelle-membrane fusion with true monomer desorption results in a stationary MOPC concentration in the membrane which is set by the magnitude of the *on* and *off* rates of the transport processes. The rate of molecular exchange is simply given by the product of the rate constant and the respective species concentration from where it originates, i.e., the bulk solution for *monomer* and micelle *on* rates, and the membrane for true monomer *off* rate. At stationary equilibrium this rate of exchange is zero and the stationary amount of MOPC

taken up by a bare membrane, for MOPC concentrations that are both below and above the CMC, is calculated from Zhelev (1996),

$$C_m = \frac{k'_{bm}}{k_{mb}} C_{\text{monomer}} + \frac{k''_{bm}}{k_{mb}} C_{\text{micelle}} \quad (3)$$

where:

- $C_m$  is the membrane concentration of MOPC (dimensionless). This quantity is measured by experiment and calculated as the mol fraction of MOPC in the membrane. It is assumed that MOPC is present in the membrane as unassociated monomer species.
- $C_{\text{monomer}}$  is the bulk solution concentration of MOPC as *monomer* (M). Up to the CMC, the solution concentration of *monomer* is given by  $C_{\text{monomer}}$ ; above the CMC it is assumed constant at 3  $\mu\text{M}$ .
- $C_{\text{micelle}}$  is the bulk concentration of MOPC as micelle (M). This quantity is the total solution concentration of MOPC minus the CMC.
- $k_{mb}$  is the *off* rate for true monomer desorption from the membrane ( $\text{s}^{-1}$ ). This quantity has been measured previously (Needham and Zhelev, 1995), and in these experiments, to be 0.3  $\text{s}^{-1}$ . *mb* represents *membrane to bulk*.
- $k'_{bm}$  is the *on* rate for MOPC *monomer* uptake ( $\text{M}^{-1} \text{s}^{-1}$ ). This quantity is unknown and a value is obtained by fitting the uptake value for the bare membrane at the CMC. *bm* represents *bulk to membrane*.
- $k''_{bm}$  is the *on* rate of MOPC micelle ( $\text{M}^{-1} \text{s}^{-1}$ ). This quantity is also unknown and a value is obtained by fitting the data.

For the rate constants, single prime (') indicates *monomer*, and double prime (") indicates micelle.

Thus for a bare lipid membrane, the first term in Eq. 3 gives the amount of MOPC taken up as *monomers* and the second term gives the amount of MOPC taken up through micelle-membrane fusion. It is seen from this equation that when the product of the rate of micelle-membrane fusion and the micelle concentration is small compared to the product of the rate of *monomer* uptake and the *monomer* concentration, the amount of MOPC transported through micelle-membrane fusion is negligible. Therefore, by reducing the micelle concentration in the bathing solution, or, as in the case of the PEG-protected bilayers, the rate of micelle-membrane fusion itself, the total amount of MOPC in the membrane can be manipulated.

The next task is to account for the retarding influence of the polymer layer on this kinetic balance and to predict the stationary equilibrium amount of MOPC taken up by the membrane as a function of the surface density of PEG(750)-

lipid. This is done by considering the association of *monomers*, the disassociation of true monomer, and the fusion of micelles to be apparent first-order reactions governed by activation energy processes (Glasstone et al., 1941). [The term "apparent" is used since we do not know exactly the form of the activation energy barrier and how many distinct barriers are in fact included in the reaction coordinate.] The *on* and *off* rates for the bare membrane will therefore depend on a barrier energy. Conceptually, we treat the polymer mushrooms as impenetrable structures, an assumption that appears valid from estimates of grafted polymer density (Torchilin et al., 1994). Access to the surface by *monomer* and micelle then is only achieved via the free surface area not occupied by the "hard-sphere" polymer mushrooms. Then, assuming that the polymer layer creates an apparent lateral surface pressure in the region next to the membrane surface, this surface pressure gives the additional contribution to the activation energy barrier to close approach and uptake of *monomers* and micelle, i.e., the *on* rates for *monomer* and micelle are modified to reflect their dependence on the presence of PEG at the membrane surface. As indicated by our data, the true monomer *off* rate does in fact not depend on PEG-lipid concentration, and, by implication, we might expect that true monomer *on* rate is also not retarded by the presence of PEG-lipid; only the *on* rate of oligomers and micelle species are affected by the PEG-lipid. Thus, strictly speaking, this excluded area approach represents one limit to the model, which must be relaxed for small molecules that can pass both through the free spaces and, at a slower rate, through the actual polymer region itself (Needham et al., 1997). In order to take this model any further it is necessary to describe the geometric characteristics (size and shape) of both the grafted PEG(750), true monomer and the MOPC micelle, and these are derived in Appendices 1 and 2.

These geometric characteristics allow us to draw to scale true monomer, MOPC micelle (spheroid,  $66 \text{ \AA} \times 86 \text{ \AA}$ ), and the PEG-lipids as mushrooms ( $R_F = 19 \text{ \AA}$ ) for a surface density equivalent to  $\sim 5 \text{ mol \%}$  PEG-lipid (Fig. 10). With these dimensions in mind, we will now discuss how the geometric features determine the contribution of the excluded area of PEG(750) mushrooms to the process of MOPC exchange with the lipid membrane in terms of an additional activation energy for close approach to the membrane.

To date, the exact process of surfactant uptake by lipid membranes is still not well understood, even for unmodified bilayers. The increase of the barrier energy due to the presence of PEG is taken to represent the additional work required to transport MOPC through the mushroom region. This work ( $W$ ) is calculated by multiplying the area in the mushroom region ( $A_{sp}$ ) to be occupied by monomer, oligomer, or micelle species, by the surface pressure ( $\Pi_{PEG}$ ) of the polymer mushrooms for a given surface density that is necessary to be overcome in order to create sufficient free surface area at the membrane interface to accommodate the adsorbing species.

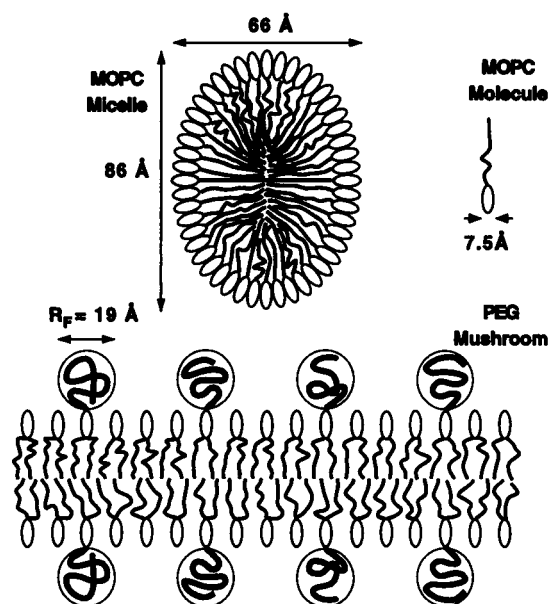


FIGURE 10 Scale drawing of a MOPC micelle at the surface of a PEG-grafted bilayer. Micelle and polymer dimensions were calculated as described in Appendices 1 and 2. The PEG-lipid density shown is  $\sim 5 \text{ mol \%}$ .

$$W = \Pi_{PEG} A_{sp} \quad (4)$$

For ideally mixed polymer lipid in liquid lipid membranes, this lateral surface pressure is inversely related to the free surface area ( $A_{free}$ ), i.e., total membrane area ( $A_{mem}$ ) minus the impenetrable area occupied by polymer mushrooms ( $A_{PEG}$ ).

$$\Pi_{PEG} = \frac{RT}{A_{mem} - A_{PEG}} \quad (5)$$

The extrinsic areas in this additional work term are then rearranged in terms of areas per molecule at the membrane surface for *monomer*, micelle, lipid, PEG, and the mol fraction of PEG-lipid in the membrane. The increase of the barrier energy then gives an exponential correction factor for the apparent decrease of the *on* rate of *monomer* uptake and micelle fusion as compared to the respective *on* rates for the bare membrane. The rates of *monomer* uptake  $k'_{bm(PEG)}$  and micelle fusion,  $k''_{bm(PEG)}$ , in the presence of PEG(750) are equal to the product of the same rates for membranes without PEG(750),  $k'_{bm}$ , and  $k''_{bm0}$  and the exponential correction factor,

for *monomer*:

$$k'_{bm(PEG)} = k'_{bm0} \exp\left(-n_{PEG} \left(\frac{a_{monomer}}{a_{lipid}}\right)\right) \quad (6a)$$

for micelle:

$$k''_{bm(PEG)} = k''_{bm0} \exp\left(-n_{PEG} \left(\frac{a_{micelle}}{a_{lipid}}\right)\right) \quad (6b)$$

where  $n_{\text{PEG}}$  is the PEG(750) molar concentration in the membrane;  $a_{\text{lipid}}$  is the area per molecule of the bilayer lipid;  $a_{\text{monomer}}$  is the area per molecule of MOPC monomer; and  $a_{\text{micelle}}$  is the cross-sectional area of the micelle projected at the surface that corresponds to the point of micelle-membrane fusion (see Fig A1 and Appendix 2). Equations (6a) and (6b) are similar to the equation used by Andrade (1985) and later by Noppl-Simson and Needham (1996) for avidin binding to biotinylated lipid vesicles. They can be extended to include the excluded area of the mushroom itself by multiplying the exponentials in Eqs. 6a and 6b by,

$$\left( \frac{1}{1 - n_{\text{PEG}}(a_{\text{F}}/a_{\text{lipid}})} \right) \quad (7)$$

where  $a_{\text{F}}$  is the apparent Flory area per PEG mushroom.

Substitution of Eqs. 6 and 7 into Eq. 3 gives the amount of MOPC in the lipid membrane at stationary equilibrium for membranes with different concentrations of grafted PEG(750) due to the uptake of both monomers and micelles,

$$C_{\text{m}} = \frac{k'_{\text{bm}0}}{k_{\text{mb}}} \cdot \exp\left(-\frac{n_{\text{PEG}}a_{\text{monomer}}}{a_{\text{lipid}}(1 - n_{\text{PEG}}(a_{\text{F}}/a_{\text{lipid}}))}\right) C_{\text{monomer}} + \frac{k''_{\text{bm}0}}{k_{\text{mb}}} \cdot \exp\left(-\frac{n_{\text{PEG}}a_{\text{micelle}}}{a_{\text{lipid}}(1 - n_{\text{PEG}}(a_{\text{F}}/a_{\text{lipid}}))}\right) C_{\text{micelle}} \quad (8)$$

In this equation, the experimentally known parameters are 1) the concentration of MOPC in the membrane  $C_{\text{m}}$  (mol fraction); 2) the concentration of PEG-lipid in the membrane  $n_{\text{PEG}}$  (mol fraction); 3) the total MOPC concentration in the aqueous solution  $C$  (M) as monomer  $C_{\text{monomer}}$  or micelle  $C_{\text{micelle}}$ ; the off rate for monomer desorption  $k_{\text{mb}}$ , equal to  $0.3 \text{ s}^{-1}$  (Needham and Zhelev, 1995, and this study); 4) the area per SOPC lipid in the membrane  $a_{\text{lipid}}$ , equal to  $65 \text{ \AA}^2$  (McIntosh and Simon, 1986); and 5) the apparent micelle area  $a_{\text{micelle}}$ , equal to  $1385 \text{ \AA}^2$ , corresponding to a critical micelle radius of  $21 \text{ \AA}$  (see Fig A1 and Appendix 2).

Two other parameters, the area per monomer  $a_{\text{monomer}}$  and the exclusion region of the polymer  $a_{\text{F}}$ , are essentially coupled and so are somewhat free parameters. That is, while the exclusion region of the polymer  $a_{\text{F}}$ , equal to  $288 \text{ \AA}^2$  as determined from the Flory radius of the PEG chain of  $19 \text{ \AA}$ , (see Appendix 1), gives an estimate of the excluded area of the polymer chain, at any one moment the polymer does not actually occupy the whole area and we cannot specify exactly the excluded area "seen" by a molecule of similar or smaller size such as true monomer or oligomer. The Flory radius is therefore an upper bound in this "hard sphere" approach for the exclusion region of the PEG mushroom. [The polymer is in fact only 17-mers and so the Flory radius itself, which is based on a random walk statistic, may not fully represent the physical size of the relatively small polymer chain.] Also, the area of the monomer has some uncertainty since the adsorbing species is really a distribu-

tion of true monomer and oligomer and so will have a value that is a weighted average between that of the true monomer cross-section of  $45 \text{ \AA}^2$  (Mattai and Shipley, 1986) and the trimer of  $60 \text{ \AA}^2$ . There is then no independent way of measuring these two characteristics, and the uptake data can in fact be fit by several different reasonable ratios (shown later in Fig. 12). For example, similar fits are obtained for a slightly smaller than calculated  $a_{\text{F}} = 254 \text{ \AA}^2$  (mushroom size of  $18 \text{ \AA}$ ) and  $a_{\text{monomer}} = 45 \text{ \AA}^2$  (size of an MOPC monomer), and for  $a_{\text{F}} = 232 \text{ \AA}^2$  (mushroom size of  $17.2 \text{ \AA}$ ), and  $a_{\text{monomer}} = 60 \text{ \AA}^2$  (size of an MOPC trimer).

Given that we can provide some reasonable estimates for the areas of the adsorbing monomer and the surface grafted polymer, the remaining unknowns in Eq. 8 are the on rates for monomer and micelle. For an off rate for true monomer measured to be  $0.3 \text{ s}^{-1}$ , the on rate for the monomer  $k'_{\text{bm}}$ , in the absence of both PEG-lipid in the membrane and micelles in the solution, can be determined by using Eq. 3 from the measured MOPC membrane uptake of  $11.1 \text{ mol } \%$  at  $3 \text{ \mu M}$  (see Fig. 4). The monomer on rate is therefore  $1.11 \times 10^4 \text{ M}^{-1} \text{ s}^{-1}$ . If we assume that this unique estimate for the monomer on rate can be used for membranes that contain PEG-lipid, and over the whole MOPC concentration range, then the only other unknown is the on rate for micelles for the bare membrane. A value for this on rate for micelles is therefore chosen such that the best fit is obtained to all the data for uptake versus the concentration of MOPC above the CMC in the bathing solution (Fig. 6) and mol % PEG-lipid in the membrane (Fig. 4). This on rate for micelles for the bare membrane is therefore found to be  $170 \text{ M}^{-1} \text{ s}^{-1}$ , and is  $\sim 65$  times smaller than for monomer.

The presence of PEG modifies these on rates further and creates an even bigger discrepancy the higher the PEG surface density. The corrections to the bare membrane on rates for monomer and micelle are given by the exponential terms in Eq. 6, and are shown in Fig. 11. In the absence of PEG,  $n_{\text{PEG}}$  is zero and so the correction is 1. For monomer, (as true monomer) the correction is only reduced to 0.8 at  $15 \text{ mol } \%$  PEG-lipid, and falls to 0.4 at  $20 \text{ mol } \%$  PEG-lipid. For trimers, the correction reduces the on rate only slightly. In our experiments we do not actually see this retardation in rate of passage through the PEG layer as discussed earlier, and so the "hard sphere" model, in reality, appears to break down at these high PEG-lipid concentrations when the free area becomes relatively small and monomers can gain access to the membrane through the actual polymer mushrooms themselves. For micelle, the equation predicts a reduction in on rate that falls rapidly, such that at  $10 \text{ mol } \%$  PEG-lipid it is 0.02 of the bare membrane value and at  $20 \text{ mol } \%$  PEG-lipid it is  $8 \times 10^{-14}$  times smaller!

Fits of the model represented by Eq. 8 are now presented in Fig. 12.

**B2.1 Model fits to data: fixed MOPC bulk concentration ( $3 \text{ \mu M}$  and  $100 \text{ \mu M}$ ); variable mol % PEG-lipid ( $0$ – $20 \text{ mol } \%$ ).** The membrane uptake data for fixed bulk solution concentrations of MOPC as a function of PEG-Lipid (up to  $20 \text{ mol } \%$ ) from Fig. 4 are again shown in Fig. 12 along with

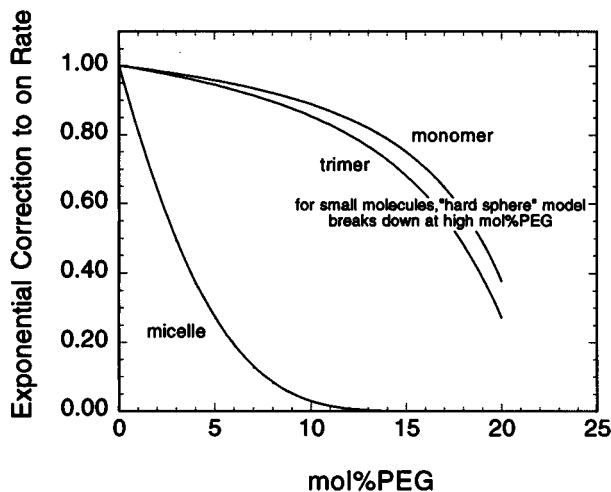


FIGURE 11 Plot of the exponential correction factor to the *on* rates (from Eq. 8) for true monomer, trimers, and micelles. When the mol % PEG-lipid is zero, the correction is 1. The *on* rate for micelles is 0.02 of the bare membrane value at 10 mol % PEG-lipid and at 20 mol % PEG-lipid is  $8 \times 10^{-14}$  times smaller. Note that, because of the possibility of transport through the polymer mushroom itself, the "hard sphere" model for *monomers* breaks down at high mol % PEG-lipid

the predictions of the stationary equilibrium model. Parameters were fixed as discussed above. This plot allows us to see the breakdown in the contributions of all species, true monomer, oligomers, and micelles. The figure consists of two sets of experimental data for 3  $\mu\text{M}$  and 100  $\mu\text{M}$  MOPC, and the theoretical fits for MOPC solution concentrations of 3  $\mu\text{M}$  (curve 2; monomer and oligomer) and 100  $\mu\text{M}$  (curve 4; all species), and the uptake due to true monomer alone [horizontal dashed line (1)] and micelles alone (dotted curve 3) for the 100  $\mu\text{M}$  case.

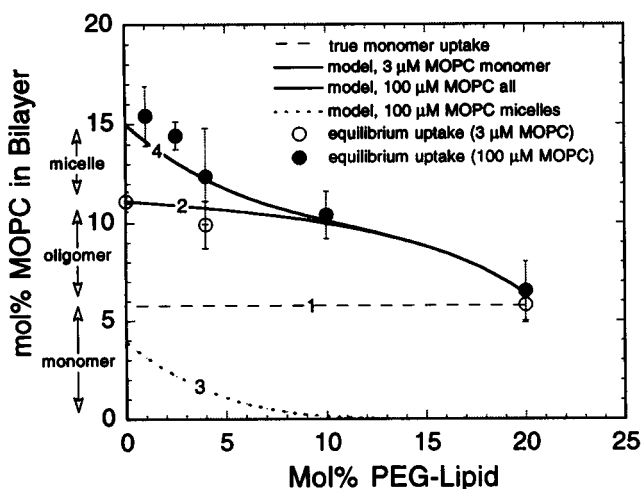


FIGURE 12 Theoretical model fitted to the data shown earlier in Fig. 4, for MOPC uptake by membranes containing different amounts of PEG-lipid from MOPC solutions of 3  $\mu\text{M}$  (open circles, curve 2) and 100  $\mu\text{M}$  (closed circles, curve 4). True monomer uptake is shown by the dashed line (curve 1). The amount of MOPC taken up as micelles is shown by the dashed curve (curve 3).

At 20 mol % PEG-lipid for both 3  $\mu\text{M}$  and 100  $\mu\text{M}$  MOPC, all but true monomer is excluded and so the horizontal dashed line (1) represents the level of true monomer uptake for all PEG-lipid concentrations at and above the CMC. For MOPC solution concentrations of 3  $\mu\text{M}$  (curve 2), there are no micelles and so Eq. 6 reduces to just the first term, and the measured uptake is fitted by considering only true monomer and oligomers as discussed above. As indicated on the figure, oligomers then account for the additional  $\sim 5$  mol % MOPC, over and above that for true monomers. For the higher 100  $\mu\text{M}$  MOPC solution concentration, as the PEG-lipid concentration in the membrane is reduced from 20 mol % to zero (curve 4), the data are coincident with uptake of *monomer* (curve 2) down to  $\sim 10$  mol % PEG-lipid. Below 10 mol % PEG-lipid, uptake of micelles (curve 3) accounts for the remaining 4 mol % MOPC taken up by the membrane.

## CONCLUDING REMARKS AND SUMMARY

Thus, while true monomers are not excluded from the membrane by the PEG(750), oligomers and micelles are, to a greater extent the more PEG-lipid there is in the membrane. This stationary equilibrium model therefore has been able to account for the MOPC uptake data in terms of the contributions made by each of the three interacting species. For maximum MOPC uptake at stationary equilibrium (1 mol % PEG-lipid, 100  $\mu\text{M}$  MOPC), true monomer accounts for  $\sim 6$  mol %, oligomers for an additional 5 mol %, and micelles for 4 mol %.

New insights into the process of micelle fusion with both the bare and PEG-covered membranes are also obtained by considering the relative magnitudes of the *on* rates for *monomer* and *micelle* as determined from this fitting of the data. For example, for the bare membrane case, if the *on* rate for micelles is calculated on a per mol of micelle basis (170 monomers/micelle), then we see that the rate of micelle fusion with the bare membrane is actually  $10^4$  times slower than that for *monomer*. This suggests that there must indeed be some activation energy for micelle break-up at the bare membrane interface that is obviously not present for simple *monomer*-membrane exchange, i.e., micelle-membrane fusion involves a transition state complex that takes some time to form.

Secondly, for the PEG-covered membrane there is an additional contribution to the activation energy for micelle-membrane fusion. The magnitude of this additional energy barrier calculated from the exponential of the second term in Eq. 6 is shown in Fig. 13. This additional work is seen to increase with increasing PEG-lipid concentration in the bilayer. At the point at which micelles are essentially excluded from access to the lipid surface, i.e.,  $\sim 10$  mol % PEG-lipid, the additional work is  $\sim 3$  kT. In contrast, the additional work to transport *monomer* across the PEG layer barely reaches kT, even at 20 mol % PEG-lipid.

In summary, we have studied the influence of grafted PEG(750) as PEG-lipids on MOPC monomer exchange and

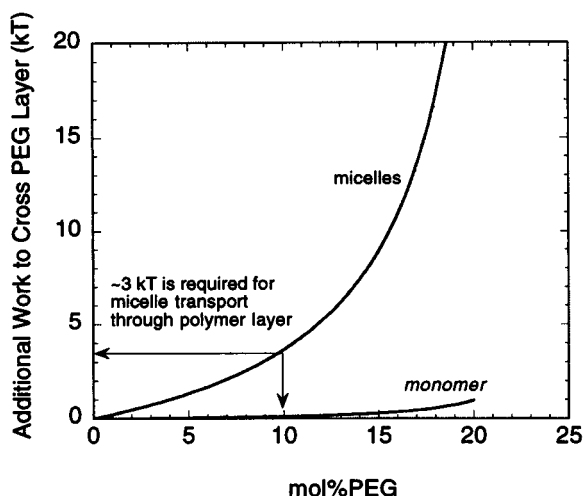


FIGURE 13 Additional work for transporting a monomer and a micelle across the grafted PEG layer for different PEG-lipid densities (as mol % in the membrane) in relation to the available thermal energy, kT. The additional work to transport the micelle increases exponentially with increasing PEG-lipid density and for a membrane with 4 mol % PEG-lipid it is on the order of kT. With an increase of PEG-lipid concentration to 10 mol %, the additional work increases to 3 kT, which corresponds to almost complete arrest of micelle-membrane fusion (see Fig. 12).

micelle fusion with lipid bilayer vesicle membranes. The experimental results and theoretical modeling show that PEG(750)-lipid has a strong inhibitory effect such that micelle-membrane fusion decreases with increasing surface density of grafted PEG(750), while true monomer uptake and desorption are not inhibited at all. At  $\sim 10$  mol % PEG-lipid, corresponding to only half-complete coverage of the membrane surface by PEG(750) mushrooms, micelle-membrane fusion was essentially prevented. The amount of MOPC in a lipid bilayer membrane can be controlled both by solution concentration and PEG grafting density. With increasing MOPC uptake by the lipid membrane, the membrane becomes progressively weaker. The experimental data are well described by a stationary equilibrium model in which *monomer* uptake and micelle-membrane fusion are considered first-order reaction processes and from which the rates for *monomer* and micelle exchange are determined to be  $10^4 \text{ M}^{-1} \text{ s}^{-1}$  and  $170 \text{ M}^{-1} \text{ s}^{-1}$ , respectively. The modeling of micelle-membrane fusion in the presence of grafted PEG(750), and the consideration of geometry characteristics of both PEG(750) mushroom and MOPC micelle, show that MOPC micelles must be in intimate contact with the headgroups of the membrane lipids in order for the fusion process to occur. The thermodynamic analysis and stationary equilibrium model both suggest that the solution properties of MOPC in the aqueous and bilayer phases are not ideal, and that MOPC is slightly aggregated, on average as trimers, in the aqueous phase below the CMC. Thus, oligomers of MOPC monomer, present in solution below the CMC, take part in the MOPC exchange and also contribute to the uptake above the CMC. An interesting finding, then, from these experiments and analysis is that the PEG

layer can actually sample the size distribution of oligomeric aggregates for these surfactant solutions. Thus, simply by changing the surface density of the thin, grafted, PEG-layer we have been able to detect the presence of pre-CMC oligomers. When the permeating species interacts with the bilayer and changes its area by only a fraction of a percent, the grafted PEG acts as a very effective molecular scale “filter” and micropipette measurements of vesicle area provide a sensitive measure of the amount and rate of passage through this filter. The combination of this PEG layer with the lipid bilayer therefore represents a versatile assay system for investigating the permeability properties of such grafted polymers to macromolecules and association colloids in the nanometer size range.

## APPENDICES

### Appendix 1. Geometric characteristics of grafted PEG polymer

PEG has been shown to be a “non-adsorbing” polymer, i.e., when vesicles are placed in a bulk polymer solution there is a depletion zone extending from the surface in which the polymer concentration is less than in the bulk solution (Arnold et al., 1987; Evans and Needham, 1988). When PEG(750) is covalently attached to a lipid molecule in the membrane, the polymer is confined to remain in a region next to the membrane surface, and, because of its non-adsorbing property, it extends away from the surface in either a “mushroom” or “brush” conformation, depending on surface density. For low polymer densities in the mushroom regime, the conformation of an individual PEG(750) chain is essentially unaffected by the presence of the other chains. In this case the polymer conformation is similar to that of a single chain in solution (deGennes, 1980). Then, the polymer will occupy a region next to the membrane surface which has an apparent size given by the Flory radius  $R_F$  (deGennes, 1980)

$$R_F = aN^{3/5} \quad (\text{A.1})$$

where  $a$  is the apparent monomer size and  $N$  is the number of monomers in the chain.

The apparent size of the PEG(750) monomer is on the order of  $3.5 \text{ \AA}$  (Kenworthy et al., 1995). The number of monomers for PEG(750) is 17. This gives a value of  $\sim 19 \text{ \AA}$  for the Flory radius. The projected area of the region corresponding to this Flory radius is  $288 \text{ \AA}^2$ . This projected area gives the area of membrane surface covered by a single PEG(750) “mushroom.” A comparison of the mushroom area to the area of a single lipid molecule [which is on the order of  $65 \text{ \AA}^2$  (McIntosh and Simon, 1986)] shows that the grafted PEG(750) is in a mushroom conformation until PEG(750)-lipid concentrations in the membrane reach  $\sim 22$  mol %, at which point the mushrooms begin to overlap and the so-called “brush” regime begins (deGennes, 1980). Therefore, in the experiments presented in this study, where PEG(750)-lipid concentrations ranged from 0.5 mol % to 20 mol %, the PEG(750) grafted to the surface was in the mushroom conformation, and essentially completely covered the lipid bilayer surface at 20 mol %.

### Appendix 2. Geometric characteristics of MOPC monomer and micelle

The size and shape of MOPC micelles have not been measured experimentally and so, for the purposes of this study, we calculate these geometric characteristics by using simple molecular shape considerations and check these considerations against surfactants for which their micelle size and shape have been measured. Israelachvili et al. (Israelachvili et al., 1980) have shown that the size and shape of lipid aggregates depend on the

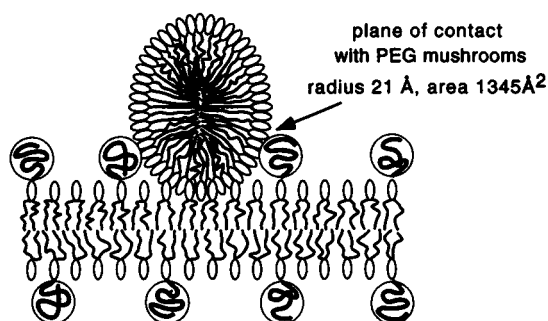


FIGURE A1 Scale drawing showing a MOPC micelle at a lipid bilayer interface with a low surface concentration of grafted PEG that just allows the micelle to come into intimate contact with the bilayer interface, i.e., headgroup intermixing. The cross-sectional area of the micelle at the plane of contact with the PEG mushrooms is  $1345 \text{ \AA}^2$ . This is the denuded area that must be created at the surface of the bilayer against the lateral surface pressure of the PEG mushrooms. The work to create this area gives rise to additional activation energy for passage of the monomer and micelle to the lipid surface as described by the exponential terms in Eq. 8.

area of the surfactant headgroup, the length of its hydrocarbon chain, and the chain volume. These molecular characteristics are used to "construct" an MOPC micelle with minimum exposed hydrophobic area. It is assumed that the micelle hydrophobic region is incompressible, does not have void space at the center, and one of the dimensions of the micelle hydrophobic core does not exceed twice the length of a lysolipid hydrocarbon chain. Because the lysolipid making up MOPC micelles is a single chain molecule, it is expected that its micelle will be axisymmetric (Benedouch et al., 1983). Also, since the cross-sectional area of a single hydrocarbon chain ( $\sim 34 \text{ \AA}^2$ ) (McIntosh et al., 1995) is smaller than the area per headgroup ( $\sim 44 \text{ \AA}^2$ ) (Mattai and Shipley, 1986), the relevant molecular area for the packing of single-chain phosphatidylcholines in micelles is the headgroup area. The apparent monomer cross-sectional diameter is then  $\sim 7.6 \text{ \AA}$ .

Before using these assumptions to calculate the size of the MOPC micelle, we test the approach and predict the size and shape of dicaproylphosphatidylcholine and diheptanoylphosphatidylcholine micelles that have been measured experimentally (Lin et al., 1987). Thus, the micelle hydrophobic core is expected to have a spheroidal shape with minor axes equal to the maximum length  $l_{\max}$  of the lipid hydrocarbon chain. The lipid hydrocarbon length is calculated from the number of hydrocarbons  $N_h$  in the chain, by using Tanford's formula (Tanford, 1980),

$$l_{\max} = (1.5 + 1.265(N_h - 1)) \text{ \AA}. \quad (\text{A.2})$$

Similarly, the volume of the hydrocarbon region  $V_h$  is calculated by Tanford (1980),

$$V_h = (27.4 + 26.9(N_h - 1)) \text{ \AA}^3. \quad (\text{A.3})$$

Using the above characteristics for dicaproylphosphatidylcholine and diheptanoylphosphatidylcholine, the minimum exposed hydrophobic area for their micelles is found when the micelles are made of 19 monomers and 26 monomers, respectively. The number of monomers per micelle (or the micelle aggregation number) for these two short-chain lipids, determined from small-angle neutron scattering experiments, is 19 and 27 (Lin et al., 1987), respectively. Thus, the aggregation numbers calculated from the geometric approach are very similar to the ones measured experimentally, and this appears to validate our approach and use of the calculation for MOPC.

The aggregation number of MOPC micelles determined by this geometric approach is 161. This aggregation number gives a micelle weight of 84,000, which is similar to the micelle weight for egg lysophosphatidylcholine of 95,000, determined from diffusion and viscosity measurements (Perrin and Saunders, 1963). The shape of the hydrophobic core of the

MOPC micelle, calculated from the model, is that of a spheroid with a minor axis equal to  $23 \text{ \AA}$  and a major axes equal to  $33 \text{ \AA}$ . The hydrophobic core is covered with lipid headgroups that extend  $\sim 10 \text{ \AA}$  from the core (McIntosh and Simon, 1986), giving final micelle dimensions of  $66 \text{ \AA} \times 86 \text{ \AA}$ , as shown in Fig. 10.

As discussed in the text, a critical area is used in the calculations (Eq. 8) for the cross-sectional area of the micelle  $a_{\text{micelle}}$  at the point at which the PEG mushrooms touch the micelle when the micelle just intercalates into the lipid headgroup region of the bilayer. As shown in Fig. A1, for the PEG750, this plane is  $\sim 10 \text{ \AA}$  from the bilayer surface, and cuts the spheroidal micelle at a radius of  $20 \text{ \AA}$ , having a cross-sectional area of  $1345 \text{ \AA}^2$ .

The authors thank Dr. Evan Evans for many stimulating discussions concerning the interpretation of the data, and Ms. Stephanie Reed for carrying out the measurements of the MOPC critical micelle concentration.

This work was supported by Grant GM 40162 from the National Institutes of Health, and D. V. Zhelev acknowledges support from the Whitaker Foundation.

## REFERENCES

- Allen, T. M. 1989. Stealth liposomes: avoiding reticuloendothelial uptake. G. Lopez-Bernstein and I. Fidler, editors. UCLA Symposium on Molecular and Cellular Biology. 89:405.
- Allen, T. M., C. Hansen, F. Martin, C. Redmann, and A.-Y. Young. 1991. Liposomes containing synthetic lipid derivatives of poly(ethylene glycol) show prolonged circulation half-lives in vivo. *Biochim. Biophys. Acta.* 1066:29-36.
- Andrade, J. D. 1985. Principles of protein adsorption. In *Surface and Interfacial Aspects of Biomedical Polymers*. J. D. Andrade, editor. Plenum Press, New York.
- Arnold, K., A. Herrmann, K. Gawrisch, and L. Pratsch. 1987. Water mediated effects of PEG on membrane properties and fusion. In *Molecular Mechanisms of Membrane Fusion*. S. Ohki, D. Doyle, T. D. Flanagan, S. W. Hui, and E. Mayhew, editors. Plenum Press, New York and London. 255-272.
- Beddu, F. K., P. Tang, Y. Xu, and L. Huang. 1996. Interaction of poly(ethylene glycol)-phospholipid conjugates with cholesterol-phosphatidylcholine mixtures. Sterically stabilized liposome formulations. *Pharm. Res.* 13:718.
- Benedouch, D., S.-H. Chen, and W. C. Koehler. 1983. Structure of ionic micelles from small angle neutron scattering. *J. Phys. Chem.* 87: 153-159.
- Carignano, M. A., and I. Szleifer. 1994. Pressure isotherms, phase transition, instability, and structure of tethered polymers in good, theta, and poor solvents. *J. Chem. Phys.* 100:3210-3223.
- Chakrabarti, A., and R. Toral. 1990. Density profile of terminally anchored polymer chains: a Monte Carlo study. *Macromolecules.* 23:2016-2021.
- Chattopadhyay, A., and E. London. 1984. Fluorimetric determination of CMC avoiding interference from detergent charge. *Anal. Biochem.* 139: 408-412.
- Chonn, A., and P. R. Cullis. 1992. Ganglioside GM1 and hydrophilic polymers increase liposome circulation times by inhibiting the association of blood proteins. *J. Lipo. Res.* 2:397-410.
- deGennes, P. G. 1980. Conformation of polymers attached to an interface. *Macromolecules.* 13:1069.
- Evans, E., and D. Needham. 1988. Attraction between lipid bilayer membranes in concentrated solutions of nonabsorbing polymers: comparison of mean-field theory with measurements of adhesion energy. *Macromolecules.* 21:1822-1831.
- Evans, E., W. Rawicz, and A. F. Hoffman. 1994. Lipid bilayer expansion and mechanical disruption in solutions of water-soluble bile acid. In *Bile Acids in Gastroenterology Basic and Clinical Advances*. A. F. Hoffman, G. Paumgartner, and A. Stiehl, editors. Kluwer Academic Publishers, Dordrecht, Boston, London. 59-68.

- Funasaki, N., S. Hada, and S. Neya. 1990. Concentration dependence of the micelle size of hexaoxyethylene glycol decyl ether as revealed by gel filtration chromatography. *J. Phys. Chem.* 94:8322–8325.
- Glasstone, S., K. J. Laidler, and H. Eyring. 1941. *The Theory of Rate Processes*. McGraw-Hill Co., New York.
- Hristova, K., and D. Needham. 1994. Influence of polymer-grafted lipids on the physical properties of lipid bilayers. *J. Coll. Int. Sci.* 168:302–314.
- Huang, L. 1992. *Journal of Liposome Research Forum on Covalently Attached Polymers and Glycans to Alter the Biodistribution of Liposomes*. 2.
- Israelachvili, J. N., S. Marcelja, and R. G. Horn. 1980. Physical principles of membrane organization. *Q. Rev. Biophys.* 13:121–200.
- Jeon, S. I., J. H. Lee, J. D. Andrade, and P. G. deGennes. 1991. Protein-surface interactions in the presence of polyethylene oxide. I. Simplified theory. *J. Coll. Int. Sci.* 142:149–158.
- Kenworthy, A. K., K. Hristova, T. J. McIntosh, and D. Needham. 1995. Range and magnitude of the steric pressure between bilayers containing lipids with covalently attached polyethylene glycol. *Biophys. J.* 68:1921–1936.
- Khul, T. L., D. E. Leckband, D. D. Lasic, and J. N. Israelachvili. 1994. Modulation of interaction forces between bilayers exposing short-chained ethylene oxide headgroups. *Biophys. J.* 66:1479–1488.
- Klibanov, A. L., K. Maruyama, V. P. Torchilin, and L. Huang. 1990. Amphipathic polyethyleneglycols effectively prolong the circulation time of liposome. *FEBS Lett.* 268:235–237.
- Kwok, R., E. A. Evans, and R. M. Hochmuth. 1980. Elastic area compressibility modulus and thermal area expansivity of large phospholipid-bilayer vesicles. *Fed. Proc.* 39:1656.
- Lasic, D., and F. Martin. 1995. Stealth liposomes. In *Pharmacology and Toxicology*. CRC Press, Boca Raton, FL.
- Lin, T.-L., S.-H. Chen, and M. F. Roberts. 1987. Thermodynamic analyses of the structure and growth of asymmetric linear short-chain lecithin micelles based on small-angle neutron scattering data. *J. Am. Chem. Soc.* 109:2321–2328.
- Mattai, J., and G. C. Shipley. 1986. The kinetics of formation and structure of the low-temperature phase of 1-stearoyl-lysophosphatidylcholine. *Biochim. Biophys. Acta.* 859:257–265.
- McIntosh, T. J., S. Advani, R. E. Burton, S. A. Simon, D. V. Zhelev, and D. Needham. 1995. Experimental tests for protrusion and undulation in phospholipid. *Biochemistry.* 34:8520–8532.
- McIntosh, T. J., A. D. Magid, and S. A. Simon. 1987. Steric repulsion between phosphatidylcholine bilayers. *Biochemistry.* 26:7325–7332.
- McIntosh, T. J., and S. A. Simon. 1986. Hydration force and bilayer deformation: a reevaluation. *Biochemistry.* 25:4058–4066.
- Needham, D., and E. Evans. 1988. Structure and mechanical properties of giant lipid (DMPC) vesicle bilayers from 20 C below to 10 C above the liquid crystal-crystalline phase transition at 24 C. *Biochemistry.* 27:8261–8269.
- Needham, D., T. J. McIntosh, and D. D. Lasic. 1992. Repulsive interactions and mechanical stability of polymer-grafted lipid membranes. *Biochim. Biophys. Acta.* 1108:40–48.
- Needham, D., T. J. McIntosh, and D. V. Zhelev. 1997. Surface chemistry of the sterically stabilized PEG-liposome: general principles. In *Liposomes: Rational Design*. A. Janoff, editor. Marcel Dekker, New York. In press.
- Needham, D., and R. S. Nunn. 1990. Elastic deformation and failure of lipid bilayer membranes containing cholesterol. *Biophys. J.* 58:997–1009.
- Needham, D., and D. V. Zhelev. 1995. Lysolipid exchange with lipid vesicle membranes. *Ann. Biomed. Eng.* 23:287–298.
- Needham, D., and D. V. Zhelev. 1996. Mechanochemistry of lipid vesicles examined by micropipet manipulation. In *Vesicles*. M. Rosoff, editor. Marcel Dekker, New York and Basel.
- Noppl-Simson, D., and D. Needham. 1996. Avidin-biotin interactions at vesicle surfaces: surface binding, cross-bridge formation, and lateral interactions. *Biophys. J.* 70:1391–1401.
- Papahadjopoulos, D., T. Allen, A. Gabizon, E. Mayhew, K. Matthey, S. K. Huang, K. Lee, M. C. Woodle, D. D. Lasic, C. Redemann, and F. J. Martin. 1991. Sterically stabilized liposomes: pronounced improvements in blood clearance, tissue disposition, and therapeutic index of encapsulated drugs against implanted tumors. *Proc. Natl. Acad. Sci. USA.* 88:11460–11464.
- Perrin, J. H., and L. Saunders. 1963. The micellar size and shape of lysolecithin. *Biochim. Biophys. Acta.* 84:216–217.
- Ruckenstein, E., and R. Nagarajan. 1975. Critical micelle concentration. A transition point for micellar size distribution. *J. Phys. Chem.* 79:2622–2626.
- Tanford, C. 1980. *The hydrophobic effect: formation of micelles and biological membranes*. John Wiley & Sons, New York.
- Tirrell, M., E. Parsonage, H. Watanabe, and S. Dhoot. 1991. Adsorbed block copolymer layers: assembly and tailoring of polymer brushes. *Polym. J.* 23:641–649.
- Torchilin, V. P., V. G. Omelyananko, M. I. Papisov, J. A. A. Bogdanov, V. S. Trubetskoy, J. N. Herron, and C. A. Gentry. 1994. Poly(ethylene glycol) on the liposome surface. On the mechanism of polymer-coated liposome longevity. *Biochim. Biophys. Acta.* 1195:11–20.
- Torchilin, V. P., and M. I. Papisov. 1994. Why do polyethylene glycol-coated liposomes circulate so long? *J. Lipo. Res.* 4:725–739.
- VanEchteld, C. J. A., B. DeKruiff, J. G. Mandersloot, and J. DeGier. 1981. Effects of lysophosphatidylcholines on phosphatidylcholine and phosphatidylcholine/cholesterol liposome systems as revealed by <sup>31</sup>P-NMR, electron microscopy and permeability studies. *Biochim. Biophys. Acta.* 649:211–220.
- Wijmans, C. M., J. M. H. M. Scheutjens, and E. B. Zhulina. 1992. Self-consistent field theories for polymer brushes. Lattice calculations and an asymptotic analytical description. *Macromolecules.* 25:2657–2665.
- Wu, N. Z., D. Da, T. L. Rudoll, D. Needham, and M. W. Dewhirst. 1993. Increased microvascular permeability contributes to preferential accumulation of stealth liposomes in tumor tissue. *Cancer Res.* 53:3765–3770.
- Yoshioka, H. 1991. Surface modification of hemoglobin-containing liposomes with polyethylene glycol prevents liposome aggregation in blood plasma. *Biomaterials.* 12:861–864.
- Zalipsky, S. 1995. Chemistry of polyethylene-glycol conjugates with biologically active molecules. *Advanced Drug Delivery Rev.* 16:157–182.
- Zhelev, D. V. 1996. Exchange of monooleoylphosphatidylcholine with single egg phosphatidylcholine vesicle membranes. *Biophys. J.* 71:257–273.